


 Cite this: *RSC Adv.*, 2024, **14**, 12817

## Current status of controlled onco-therapies based on metal organic frameworks

 Yixuan Yang and Xiaofeng Dai \*

Despite consecutive efforts devoted to the establishment of innovative therapeutics for cancer control, cancer remains as a primary global public health concern. Achieving controlled release of anti-cancer agents may add great value to the field of oncology that requires the involvement of nanotechnologies. Metal organic frameworks (MOFs) hold great promise in this regard owing to their unique structural properties. MOFs can act as superior candidates for drug delivery given their porous structure and large loading area, and can be prepared into anti-cancer therapeutics by incorporating stimuli-sensitive components into the ligands or nodes of the framework. By combining through chemical and physical features of MOFs favorable for onco-therapeutic applications and current cancer treatment portfolios taking advantages of these characteristics, this review classified MOFs feasible for establishing controlled anti-cancer modalities into 6 categories, outlined the corresponding strategies currently available for each type of MOF, and identified understudied areas and future opportunities towards innovative MOF design for improved or expanded clinical anti-cancer applications.

Received 15th January 2024

Accepted 11th March 2024

DOI: 10.1039/d4ra00375f

[rsc.li/rsc-advances](http://rsc.li/rsc-advances)

## 1 Introduction

Cancer still remains as a core public health threat worldwide, with 609 820 death incidences estimated in the United States in 2023 according to the latest cancer statistics.<sup>1</sup> Despite consecutive reports on innovative anti-cancer strategies such as immunotherapies, the cancer recovery rate has not undergone a rapid increase as a result of unresolved clinical impediments such as unavoidable adverse effects and limited treatment efficacy. These issues could be, at least partially, resolved if the drug release profile was under appropriate control, leading to an unmet need of bringing in interdisciplinary technologies such as nanomaterials.

Nanomedicine has received significant research interest in the field of oncology due to its structural and functional diversity, among which metal organic frameworks (MOFs) are of particular attractiveness. MOFs, composed of organic linkers and metal nodes, represent a novel class of crystalline porous materials featuring large porosity, an extremely high surface area (typically ranging from 1000 to 10 000 m<sup>2</sup> g<sup>-1</sup>), tunable pore size (typically 0–3 nm, up to 9.8 nm) and flexible functionality.<sup>2,3</sup> With these biologically favorable characteristics, MOFs have gained extensive and increasing attention as versatile systems for many medical applications during the past two decades such as drug delivery<sup>4–9</sup> and onco-therapeutic agents.<sup>10,11</sup> Specifically, MOFs are ideal vehicles for delivering various agents due to their

adsorption characteristics empowered by their unique metal-core hybrid and precise porous structure. The cargoes can be loaded *via* surface loading (*i.e.*, coordination through –COOH, –HSO<sub>3</sub>, –PO<sub>4</sub>, or adsorption through electrostatic interaction, hydrogen bonding, π–π stacking, *etc.*), pore loading (*e.g.*, metal nanoparticles, photosensitizer, photothermal agents, *etc.*), covalent binding (*e.g.*, –CHO, –SH, –OH, –NH<sub>2</sub>, –N<sub>3</sub>, *etc.*) and the confinement effect (*e.g.*, proteins, nucleic acids, nanoparticles larger than the pores) (Fig. 1), and the cargo-loading ratio can be determined by the properties of the agents to be loaded such as the molecular weight, hydrophilicity and size.<sup>12–16</sup> The cargo release profiles can be easily tuned by functionalizing or tailoring MOF-based drug carriers.<sup>5–9,17,18</sup> In addition, MOFs can directly serve as anti-cancer agents in response to external stimuli for controlled therapeutics if the ligands of the framework were incorporated with bioactive species such as metal-porphyrins, photosensitizers, photothermal agents and acoustically sensitizing agents, or the nodes of the framework were designed to be, *e.g.*, Fe for magnetic therapy<sup>10,11,19–22</sup> (Fig. 1).

Despite some already existing reviews on MOFs for cancer treatment that have classified MOFs in distinct ways such as by the delivery cargo,<sup>23</sup> structural components,<sup>24</sup> and synthetic approach,<sup>25</sup> we focused on controlled onco-therapeutics relying on MOFs, and classified MOFs into 6 categories, *i.e.*, pH-responsive, glutathione (GSH)-responsive, magnetism-responsive, light-responsive, temperature-responsive, and ultrasound-responsive, following their mechanisms of action. Accordingly, we discussed the therapeutic potential of these MOFs in functioning as the drug nano-carrier targeting tumor cells and/or the tumor microenvironment (TME) taking

National Local Joint Engineering Research Center for Precision Surgery & Regenerative Medicine, Shaanxi Provincial Center for Regenerative Medicine and Surgical Engineering, The First Affiliated Hospital of Xi'an Jiaotong University, Xi'an 710061, P.R. China. E-mail: xiaofengteam@163.com



advantages of the acidity and redox properties of the targets, as well as in acting as anti-cancer agents sensitive to external physical perturbations. *Via* combing through current cancer treatment portfolios taking advantages of the unique structural features of MOFs for controlled drug delivery and anti-cancer effect, we raised questions on understudied topics that may lead to the establishment of innovative anti-cancer modalities possibly revolutionizing the current cancer treatment paradigm.

## 2 MOF classification by mechanisms of action

One of the key benefits of applying MOFs for cancer control is to allow controlled release of anti-cancer agents under physical or chemical stimuli such as pH, redox level, magnetic field, light, heat and ultrasound, the outcome of which can be attributed to the relatively weak coordination bonds formed between metal ions and organic ligands within MOFs<sup>26,27</sup> (Fig. 2).

### 2.1 pH-responsive MOFs

The dominant role of anaerobic fermentation reprograms the metabolism of cancer cells towards abnormal lactate



Yixuan Yang

*Yixuan Yang focuses on biomedical applications based on biomimetic nanomaterials, including the detection of tumor markers and drug delivery *in vivo*. Yixuan Yang has been involved in publishing 5 papers in recent years.*

accumulation in the TME, known as one hallmark of cancers.<sup>28</sup> Besides, the pH of lysosomes and endosomes within tumor cells are between 4.5 and 6.3.<sup>29</sup> Thus, pH-responsive MOFs may release cargoes within tumor cells and their acidic TME milieu for targeted therapeutics if the nano-framework could be degraded under the acidic environment. This is perhaps the simplest strategy for MOF-based therapeutic design for targeted cancer control.

Drugs and ligands loaded onto MOFs generate covalent,<sup>30</sup> ionic,<sup>31</sup> and hydrogen<sup>32</sup> bonds that are sensitive to pH. Example bonds employed in MOF structural design include ether,<sup>33</sup> epoxy,<sup>34</sup> Schiff base,<sup>35</sup> and amide<sup>36</sup> bonds, all of which could be hydrolyzed in an acidic environment as a result of charge reversal and electrostatic repulsion.<sup>37</sup> For instance, CAU-1, a porous hydrostable MOF, presented abundant -OH and -NH<sub>2</sub> groups on the surface that was strongly and positively charged; CAU-1 exhibited excellent saturated adsorption capacity of tinidazole (TNZ) (approximately 450 mg g<sup>-1</sup>) attributable to the H-bond and electrostatic interactions, and released TNZ molecules under simulated physiological conditions that was controllable *via* adjusting pH of the solution.<sup>38</sup>



Xiaofeng Dai

*Xiaofeng Dai focuses on the establishment of cold atmospheric plasma based onco-therapeutic strategies against highly malignant tumors, and identification of novel biomarkers for characterizing tumors feasible for such treatments. Dr Dai was awarded with Academician of the European Academy of Natural Sciences in 2023 and Outstanding Engineer Award (Young Award) in 2022.*

*Dr Dai's has published 98 papers in the past few years, with the accumulated impact factor being 642 (highest IF = 31.281, 14 with IF >10). Dr Dai has 2 granted USA patents of invention, 4 granted Chinese patents of invention, 3 granted Chinese patents of utility, 2 granted Chinese patents of design, and 10 Chinese software copyrights as the first inventor. She holds two national scientific research funds (surface projects), and one national major project in China. Dr Dai is currently a committee member of the Chinese Society for Systems Biology (branch of Functional Genomics and System Biology), Chinese Anti-cancer Association (professional committee of Tumor Biomarkers), Biomedical Engineering Society in Jiangsu Province (professional committee of Bioinformatics), Chinese bioengineering society (professional committee of Computational Biology and Bioinformatics), and a member of Chinese Artificial Intelligence Society, Chinese Anti-cancer Association, Chinese Chemistry Society, Chinese Bioengineering Society, Biochemistry and Molecular Biology Society in Jiangsu Province, and Engineering Society in Wuxi.*



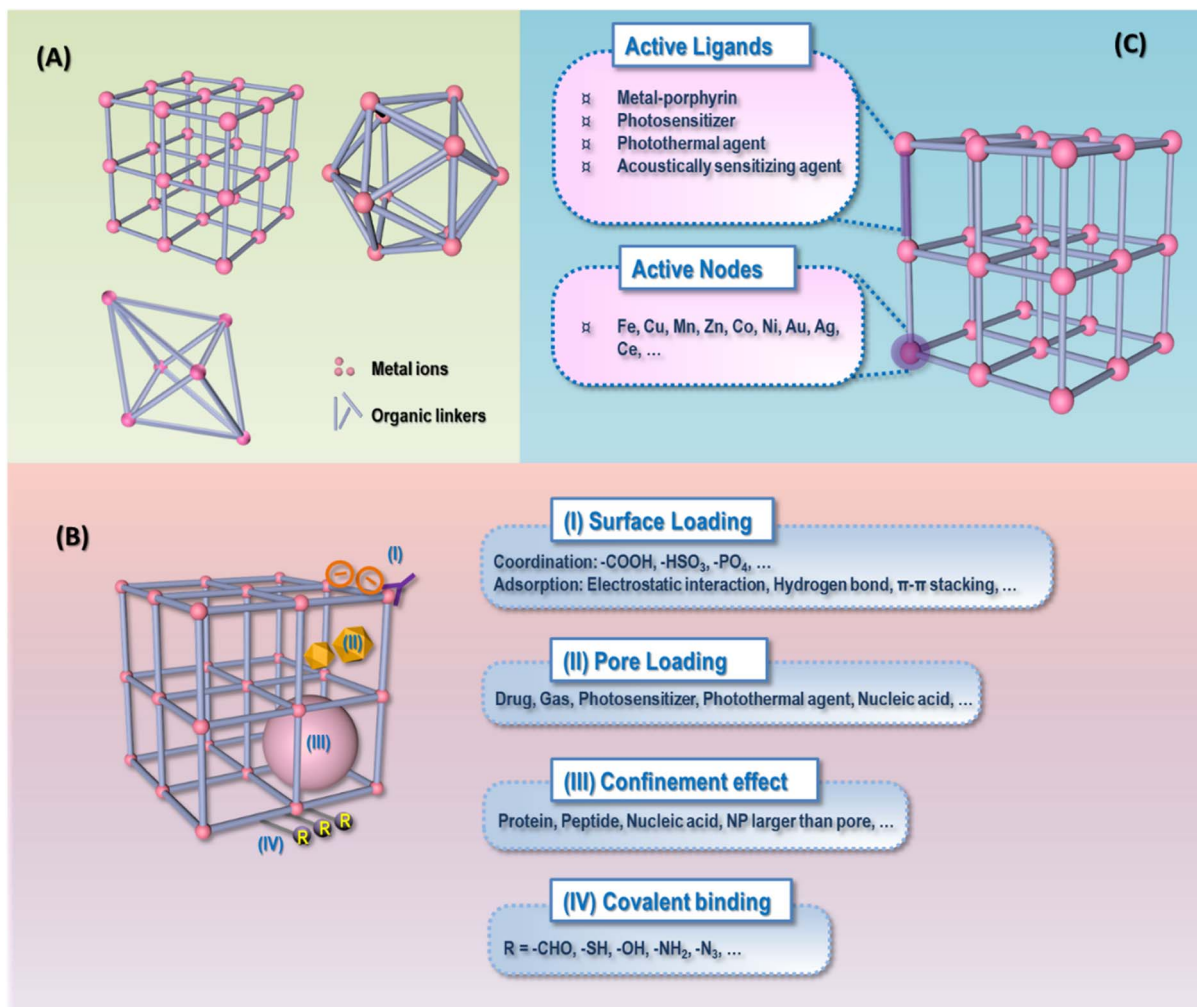


**Fig. 1** Structure of MOF and common strategies for loading MOFs with drugs and using MOFs as anti-cancer agents. (A) MOF structure. (B) Common strategies for loading MOFs with anti-cancer drugs. There exist four common strategies, *i.e.*, surface loading, pore loading, covalent binding and confinement effect. In surface loading, drugs can be loaded *via* coordination and adsorption such as electrostatic interaction, hydrogen bond or  $\pi-\pi$  stacking; in pore loading, anti-cancer agents, gases or photosensitizers etc. can be encapsulated into the pores of MOFs; in covalent binding, covalent binds can be formed *via*, *e.g.*,  $-\text{CHO}$ ,  $-\text{SH}$ ,  $-\text{OH}$ ,  $-\text{NH}_2$ ,  $-\text{N}_3$ ; in confinement effect, anti-cancer agents with the size larger than that of the pores can be incorporated. (C) Common strategies for using MOFs as anti-cancer agents. Anti-cancer agents can be incorporated into MOFs as active ligands or active nodes.

Zeolite imidazolate framework (ZIF) is comprised of metal ions (zinc or cobalt) and imidazolate linkers in tetrahedral coordination surrounded by nitrogen atoms from the five-membered imidazole ring serving as the bridging linker. ZIF is advantageous over zeolites for drug design due to its more flexibility for surface modification, higher porosity, larger surface area, and higher stability.<sup>39</sup> Among members of the ZIF family, ZIF-8 is commonly used to establish pH-sensitive drug delivery systems due to its decomposability under the acidic conditions.<sup>40,41</sup> However, the conventional structure of ZIF-8 suffers from poor stability, low water solubility and short blood circulation duration *in vivo*.<sup>42,43</sup> A plethora of studies have devoted to resolve this problem. For example, by coating hyaluronic acid (HA) on the surface of curcumin-carrying ZIF-8, Yu *et al.* fabricated Cur@ZIF-8@HA that reduced curcumin release from 32.4% to 30.6% at pH = 5.5 and further to 16.7% at pH =

7.4 within 10 h as compared with Cur@ZIF-8, suggesting the protective role of HA against early cargo leakage that may help prolong the circulation time of the nanoparticle for minimized side effects.<sup>44</sup>

Besides zinc-MOF, many other MOFs have been fabricated into pH-responsive frameworks. For instance, Zhang *et al.* proposed a syphilis mimetic TP0751-peptide decorated stem cell membrane-coated copper-based MOF (TP-M-Cu-MOF) and its use in delivering siRNAs for treating small cell lung cancers metastasized to the brain; the pH sensitivity of this Cu-MOF nanocomposite facilitated its endosomal disruption, and the cell membrane coating enabled it with a good biocompatibility, high blood-brain barrier transcytosis, and targeted brain tumor cell uptake; the results showed that by encapsulating siATP7a, this Cu-based MOF (siATP7a@TP-M-Cu-MOF) effectively silenced the target gene and triggered cancer cell cuprosis.<sup>45</sup>

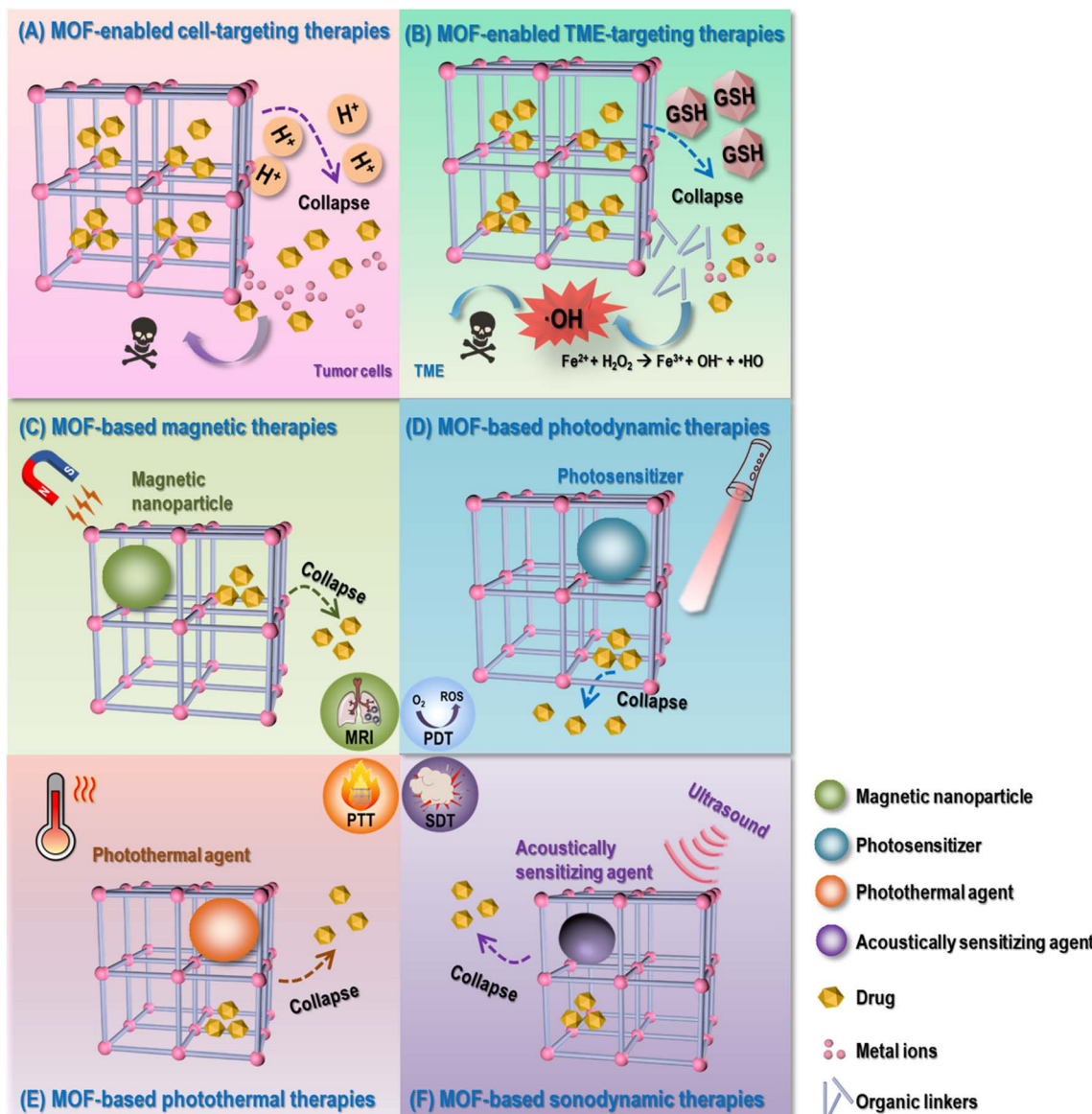


**Fig. 2** Classification of MOFs for cancer treatment based on their mechanisms of action and current therapeutic modalities sensitive to external stimuli. Most MOFs for controllable cancer treatment act as drug delivery vehicle and/or anti-cancer agent. Molecules with anti-cancer roles such as chemotherapies, gases, peptides or nucleic acids can be loaded into MOFs that decompose (A) in cancer cells or (B) in the TME to release its cargoes in a pH- or GSH-responsive manner, which is also named chemodynamic therapy or gas therapy. Bio-reactive species such as (C) magnetic nanoparticles, (D) photosensitizers, (E) photothermal agents, and (F) acoustically sensitizing agents can be loaded or incorporated into MOFs that take on actions in response to external physical stimuli such as magnetism, light, heat, and sound.

Wang *et al.* synthesized a cationic polymer (MV-PAH) and used it to modify a newly designed pH-responsive Fe-MOF nano-reactor (DOX@Fe-MOF@PEM); in this design, the poly-electrolyte multilayer (PEM) disassembled in the acidic TME to release doxorubicin (DOX) and MV-PAH, which improved the anticancer effect of DOX by generating hydrogen peroxide ( $H_2O_2$ ) and catalyzing it to hypotoxic hydroxyl radical ( $\cdot OH$ ) in the presence of intracellular  $Fe^{2+}$  (Fenton-like reaction).<sup>46</sup> Yang *et al.* proposed the use of a chitosan-coated Zn/Co-MOF as the carrier of DOX and modified it with arginine-glycine-aspartic acid functionalized gold nanoparticles (namely Zn-Co ZIF@DOX-CS-Au-RGD, abbreviated as ZD-CAR) for

photothermal (PTT) in treating liver cancers; this nanocomposite was cleaved in the acidic TME to release DOX and  $Co^{2+}$  on accurate recognition of the tumor loci by RGD; while  $Co^{2+}$  catalyzed the conversion of  $H_2O_2$  to oxygen resulting in alleviated tumor hypoxia, DOX induced cancer cell apoptosis, and Au nanoparticles converted light energy to heat under 808 near-infrared (NIR) irradiation towards enhanced tumor cell killing.<sup>47</sup>

## 2.2 GSH-responsive MOFs

Cancer cells typically have a higher redox level than their healthy peers and are thus more sensitive to oxidative

perturbation-triggered cell death. GSH is one of the most potent anti-oxidant in cells, elevated level of which is typically associated with high cancer malignancy, tumor progression and drug resistance.<sup>48</sup> MOFs degradable under GSH or sensitive to high levels of GSH can be used for treating advanced cancer cells. For example, by loading the O<sub>2</sub>-producing prodrug (platinum<sup>4+</sup>-diazido complex) into Cu<sup>2+</sup> carboxylate-based MOF (MOF-199) followed by encapsulating it with TBD (an aggregation induced-emission photosensitizer)-conjugated polyethylene glycol, Wang *et al.* fabricated TBD-Pt(iv)@MOF-199, where MOF-199 efficiently consumed intracellular GSH and released Pt(IV) that generated O<sub>2</sub> on light irradiation, resulting in synergistic image-aided photo-chemo therapy with desirable anti-cancer efficacies yet mitigated side effects.<sup>49</sup> Similarly, a Mn-based multi-targeted GSH-sensitive drug delivery system was developed to reverse cisplatin (CDDP) resistance in ovarian cancers. In this nano-carrier, Mn-based MOFs containing niraparib (Nira) and CDDP alongside transferrin (Tf) conjugated to the surface (*i.e.*, Tf-Mn-MOF@Nira@CDDP), was developed, which released Nira and CDDP in response to GSH; and Nira synergized with CDDP in inducing cancer cell apoptosis that was not achieved by using CDDP alone.<sup>50</sup> Some efforts have been devoted to establish MOFs with dual sensitivities to both pH and GSH. For instance, an Zr-MOF functionalized with acetaldehyde-modified-cystine (AMC) was formed (Zr-MOF/AMC) that successfully released methotrexate for treating cancers under both acidic and/or high GSH conditions; the mechanism was attributed to the hydrolyzation and broken of the -C=N- bonds of AMC under the acidic condition, and the cleavage of AMC disulfide bonds (-S-S-) when encountering thiols in GSH.<sup>51</sup>

### 2.3 Magnetism-responsive MOFs

Although acidic intra- and extra-cellular environments and high redox sensitivity of transformed cells offer us some natural properties for cancer targeting, pH- and GSH-responsive MOFs may fail in some real clinical cases due to the highly personalized features of these internal factors.<sup>52</sup> Physical external factors such as magnetic field, light, heat and ultrasound may avoid these problems as they are non-invasive, simple-to-use, and easy-to-control.

Magnetism-responsive MOFs represent one solution to these aforementioned issues taking advantages of external stimuli.<sup>53</sup> By transforming the magnetic field's external energy into the mechanical force effect, magnetic heating effect, and magnetic resonance signal amplification, magnetic nanoparticles (MNPs) including magnetic-responsive MOFs can manipulate various cell functionalities such as cell death, adhesion, migration and differentiation.<sup>54</sup> If MOFs were encapsulated with anti-cancer agents, they may function as both drug vehicles and MNPs towards synergized anti-cancer effect. For example, by conjugating Fe<sub>3</sub>O<sub>4</sub> MNPs with MIL-88B-NH<sub>2</sub>, MOF structures using optimized synthetic media (which contains acetic acid as a modulating agent and F127 co-polymer as a stabilizing agent), Attia *et al.* successfully produced a well-controlled hybrid magnetic nanocomposite; by loading carmustine and

mertansine, two drugs against glioblastoma, into the pores of this MOF nanocomposite, they achieved significant cancer cell toxicity yet limited side effects.<sup>55</sup>

### 2.4 Light-responsive MOFs

Light-responsive MOFs can be fabricated by encapsulating photosensitizers to the porous structures of MOFs, which take on actions by transforming external light energies into internal chemical or thermal energies, leading to the collapse of MOF structures, the ignite of photodynamic (PDT) or PTT effects, and their possible synergies.<sup>37</sup>

Among the varied light sources, near-infrared II (NIR-II), with the wavelength range being 1000–1700 nm, has been extensively used for inducing MOF structure decomposition given its superior biocompatibility and desirable penetration in-depth.<sup>56</sup> For example, by fabricating an NIR-II-photothermal palladium nanosheet core and a porphyrin-palladium MOF shell together (Pd-MOF) and loading it with large amount of PdCO (carbon monoxide with singleton palladium), Yao *et al.* created Pd@PdCO-MOF that released CO after NIR-II photo-activation and killed cancer cells through synergizing CO-based cell cytotoxicity with PTT.<sup>57</sup> Besides NIR-II, other light sources such as ultraviolet light have also been used for inducing MOF collapse which, although has excellent penetration in-depth and MOF destabilization efficacy, are clinically irrelevant given their devastating cell toxicity. To overcome this issue, a recent study reported a MOF design responsive to green light stimulation. Specifically, a UiO-AZB-F framework containing 4,4'-(diazene-1,2-diy)bis(3,5-difluorobenzoic acid) (AZB-F) as the linker (the core element responsive to green light induction) and fluorinated azobenzene as part of the backbone, was designed, which demonstrated controlled cargo release and low cell toxicity.<sup>52</sup>

### 2.5 Temperature-responsive MOFs

Temperature-responsive MOFs can be constructed by incorporating temperature-sensitive materials into the porous framework of MOFs that take on actions in response to the change of temperature.

Though functioning similarly with light-responsive MOFs, little effort has been devoted to apply temperature-responsive MOFs to fight against cancers. Current studies in this field are largely limited to, *e.g.*, enzyme immobilization, water capture, and biocatalysis. Specifically, Qiao *et al.*, modified the MOF structure with a temperature-sensitive polymer poly(*N*-isopropyl-acrylamide) (PNIPAM) through the linker dimethylvinylloxazolinone (VDMA), and immobilized this temperature-sensitive MOF on the P(NIPAM-*co*-VDMA) chains to form polymer-MOF@enzymes-based nano-reactors. By inducing the confinement effect and forming a soft nest at a high temperature, this MOF provides a tailororable space for immobilizing enzymes such as glucose oxidase, horseradish peroxidase, trypsin, cytochrome c, and glutaminase.<sup>58</sup> Also using PNIPAM as the temperature-sensitizer, Karmakar *et al.* reported an *in situ* polymerization strategy that exhibited an unprecedented temperature-controlled water capture and



release by incorporating PNIPAM into the cavity of a mesoporous MOF, MIL-101(Cr).<sup>59</sup> Chen *et al.* fabricated a temperature-responsive MOF, *i.e.*, dimethylammonium zinc formate ( $[(\text{CH}_3\text{NH}_2)_2\text{Zn}(\text{HCOO})_3]$ , DMZnF), and used it as a homogeneous catalyst to produce hydrogen from dehydrogenation of *N,N*-dimethylformamide and  $\text{H}_2\text{O}$  at 120 °C.<sup>60</sup>

## 2.6 Ultrasound-responsive MOFs

A single MOF has limited ultrasound sensitivity as a result of rapid recombination of electron holes between its structures. The responsiveness of MOFs can be effectively improved by adding another semiconductor structure to form an interface effect, which can substantially improve the sonocatalytic performance of the nanocomposite by guiding electron transfer and energy change. This would lead to reduced energy required for oxygen activation, and oxygen attracted at an excited state in response to ultrasound by gaining more electrons could rapidly produce a large amount of reactive oxygen species (ROS) to kill cancer cells.<sup>61,62</sup>

Ultrasound-responsive MOFs can be fabricated by incorporating acoustically sensitizing agents to MOFs. Pan *et al.* proposed a MOF-derived double-layer hollow manganese silicate nanoparticles (DHMS) capable of generating ROS under ultrasound irradiation, where the presence of Mn in DHMS was the key for increased ROS yield.<sup>63</sup> Another study established a defect-rich Ti-based MOF (namely D-MOF(Ti)) capable of increasing ROS generation as compared with  $\text{TiO}_2$  (a commonly used sonosensitizer) taking advantages of its narrow bandgap for improved ultrasound-triggered electron–hole separation; in addition, D-MOF(Ti) exhibited the Fenton-like activity to enable chemodynamic therapy due to the existence of  $\text{Ti}^{3+}$  ions; thus, D-MOF(Ti) simultaneously induced the Fenton-like reaction and ROS-triggered cell toxicity towards synergized onco-therapeutic outcome and, importantly, was cleared out of the body after completion of the treatment without showing any off-target effect.<sup>64</sup>

Despite these aforementioned successes, massive ROS generation and development of sonosensitizer systems including the straightforward sound-sensitive devices remain challenging.

## 3 MOF-based therapeutics

### 3.1 MOF-enabled cell-targeting therapies

Targeted therapy refers to the use of drugs to precisely identify and attack certain types of cancer cells. As MOFs can help achieve controlled cargo release under, *e.g.*, acidic or hypoxia conditions, they can be used for targeted therapy once loaded with drugs for, *e.g.*, chemotherapeutics. In addition, MOFs can help reduce the possible off-target effects of existing targeted therapies and immunotherapies by adding another layer of cancer-associated information, *i.e.*, distinct acidic or redox levels from normal cells. Thus, with the aid of MOFs, the concept of targeted therapy can be easily extended to other treatment regimens such as chemotherapies and immunotherapies for improved therapeutic outcomes with reduced adverse effects.

MOFs carrying various chemotherapeutics such as dihydroanemisinine (DHA),<sup>65</sup> DOX,<sup>17,66</sup> 5-fluorouracil (5-FU),<sup>17,67</sup> paclitaxel,<sup>68</sup> CDDP,<sup>69</sup> and oridonin,<sup>70</sup> have been consecutively reported for cancer treatment with improved therapeutic efficacies. For instance, Yan *et al.* encapsulated DHA in a pH-sensitive ZIF-8-based MOF (DHA@ZIF), and demonstrated its superiority over free DHA in many anti-cancer indexes using ovarian cancer as the tumor model.<sup>65</sup> Ling *et al.* loaded DOX and 5-FU on the surface of upconversion nanoparticles (UCMOFs) through the reactions of Schiff bases and electrostatic adsorption that showed enhanced cytotoxicity over UCMOFs@DOX and UCMOFs@5-FU under acidic conditions, indicating a successful pH-controlled release of both agents in tumor cells by this nanocomposite.<sup>17</sup> A more complicated example constructed polydopamine (PDA)-cloaked pH-responsive Fe-based MOFs loaded with D-arginine, glucose oxidase (GOX) and tiazapazamine (TPZ). In this design, GOX catalyzed the conversion of glucose and  $\text{O}_2$  into  $\cdot\text{OH}$  and gluconic acid, which blocked the nutrient supply of cancer cells and generated additional cytotoxic  $\cdot\text{OH}$ ; MOFs collapsed in the acidic environment to release TPZ and  $\text{Fe}^{3+}$  that reacted with  $\text{H}_2\text{O}_2$  towards elevated ROS production and cell killing; and the PDA coating was used to graft folate bovine serum albumin for improved tumor site targeting.<sup>71</sup>

Some MOF-enabled targeted therapies are also immunotherapeutics if the cells targeted were from the immune system. For instance, Li *et al.* proposed a MOF-based lactate-catalyzed chemodynamic approach to activate the genome editing of signal-regulatory protein alpha (SIRP $\alpha$ ) for polarizing TAMs towards the anti-cancer state. In this system, lactate oxidase (LOX) and clustered regularly interspaced short palindromic repeat-mediated SIRP $\alpha$  genome-editing plasmids were wrapped together in a pH-sensitive MOF; on acidic pyruvate activation as a result of LOX-catalyzed lactate oxidation, the genome-editing tool was released to block SIRP $\alpha$  signaling that synergized with lactate exhaustion towards promoted TAM M1 polarization.<sup>72</sup>

### 3.2 MOF-enabled TME-targeting therapies

The TME has been considered with critical roles in cancer initiation and progression and been attracted lots of attention in the design of onco-therapies. Due to the hypoxic condition of the TME, efforts have been made to take advantages of the decomposition feature of some MOFs under high GSH levels for rewiring ‘cold’ tumors to the ‘hot’ state. For example, by encapsulating the immunosuppressive enzyme indoleamine 2,3-dioxygenase inhibitor BMS-986205 and NO donor s-nitrosothiol groups (SNAP) using a GSH-sensitive MOF, Du *et al.* obtained BMS-SNAP-MOF that collapsed in response to GSH, leading to the release of BMS-986205 and abundant NO production; this synergistically resulted in increased  $\text{CD8}^+$  T cell infiltration and a decreased level of T regulatory cells.<sup>73</sup>

If Fe-based MOFs were used for targeting the TME, they are likely to be called chemodynamic therapy (CDT). The anti-tumor effect of CDT is largely dependent on the TME-responsive Fenton or Fenton-like reactions that produce  $\cdot\text{OH}$  from  $\text{H}_2\text{O}_2$ . MOF-aided CDT outweighs traditional CDT in



producing higher levels of  $\text{H}_2\text{O}_2$  for improved efficacies. For instance, Rao *et al.* fabricated BSO&OXA@MOF-LR, using which they significantly improved the survival rate of 4T1 tumor xenograft mice. In this design, the chemotherapeutic drug oxaliplatin (OXA) and buthionine sulfoxide amine (BSO) capable of blocking GSH biosynthesis were loaded to a Fe-based MOF coated with lipid bilayer (L) and edited RGD (R). While BSO blocked GSH biosynthesis and OXA took on its anti-cancer role, the L and R coating enhanced the tumor homing accuracy of these nanoparticles.<sup>74</sup> As another good example, Gong *et al.* proposed the use of  $\beta$ -lapachone ( $\beta$ -Lap), a substrate of quinone oxidoreductase 1 (NQO1), in treating NAD(P)H: NQO1<sup>high</sup>CAT<sup>low</sup> endometrial cancers. In this strategy, along with the absence of NADH, NQO1 catalyzed  $\beta$ -Lap to produce excess  $\text{H}_2\text{O}_2$  that was converted to highly active  $\cdot\text{OH}$  by RGD-functionalized nMIL-100 (*i.e.*, a Fe-based MOF sensitive to redox fluctuation) towards the trigger of oxidative stress and death of NQO1<sup>high</sup> cancer cells.<sup>75</sup> In another study, Li *et al.* created an GSH-sensitive Fe-based MOF nanoreactor (DHA@MIL-101) and used it to load DHA that was effectively accumulated in the TME to rewire TAMs towards the anti-cancer M1 state.<sup>18</sup> Also, another team developed an iron-doped folic acid (FA) modified ZIF-8 and loaded it with GOX, L-Arginine (L-Arg), and DOX to obtain GLDFe/Z-FA, which induced tumor starvation by consuming glucoses and converting endogenous  $\text{H}_2\text{O}_2$  to  $\cdot\text{OH}$  for CDT.<sup>76</sup>

If encapsulated agents in MOFs were replaced with gas signaling molecules such  $\text{O}_2$ ,  $\text{H}_2\text{S}$ , NO, and CO, they are given a new name, gas therapy.<sup>77</sup> High concentration ( $\mu\text{M}$  to  $\text{mM}$ ) of NO and  $\text{H}_2\text{S}$  have strong cytotoxicity and CO fights against cancer cells due to its ability to reverse drug resistance and increase the chemo-sensitivity of cancer cells.<sup>78,79</sup> Gas molecules are superior to chemical agents in being easily exhaled out of the body due to their smaller size, more effective diffuse ability across cell membranes and the blood-brain barrier, and less likelihood of being accumulated in the body and causing toxicity. However, gas molecules must be delivered under strict supervision and control given their short life spans, high dependence on concentration, and site specificity,<sup>80,81</sup> where MOFs may act as an ideal nano-carrier. By loading a biocompatible NO donor and L-Arg to a Fe-based MOF, *i.e.*, (PCN)-223-Fe, Ji *et al.* fabricated L-Arg@PCN-223-Fe that sustainingly released L-Arg to react with Fe-porphyrin in PCN-223-Fe for sufficient NO generation and drug resistance reversal at the expense of  $\cdot\text{OH}$  present in the TME.<sup>82</sup> In addition, peroxynitrite ( $\text{ONOO}^-$ ), a highly active molecule with a significant anti-cancer cytotoxicity, can be produced during the interactions between NO and superoxide free radicals. Xia *et al.* developed a GSH-responsive NO-generating nanosystem to boost ROS production through GSH depletion and hypoxia relief. Specifically, they wrapped nicorandil (Nic) into the porphyrinic MOF nanoparticles, and coated it with HA through electrostatical adsorption to target cells over-expressing CD44 and prevent Nic leakage. In this nano-system, Nic reacted with GSH to produce NO towards improved  $\text{O}_2$  supply and sufficient ROS production, the generated NO reacted with  $\cdot\text{OH}$  to produce highly reactive  $\text{ONOO}^-$  that together with the residual  $\cdot\text{OH}$  and NO killed cancer cells.<sup>83</sup>

### 3.3 MOF-based magnetic therapies

MOF-based magnetic therapy, here, refers to a therapy where tumor killing is achieved by incorporating MNPs into MOFs and exposing magnetism-responsive MOFs to an appropriate alternating magnetic field (AMF) taking advantages of the magneto-thermia effect.<sup>84</sup> Specifically, an AMF was able to remotely actuate the magneto-hyperthermia effects by increasing the temperature up to over 43 °C, mainly attributing to the magnetic energy released from Brown and Néel relaxation.<sup>85</sup> As transformed cells are featured with disorganized vascular network, they suffer from decreased convective cooling rate as a result of reduced blood flow than their healthy peers, leading to hampered ability in dissipating additional heat. This gives us the opportunity to kill cancer cells taking advantages of the differential sensitivity of transformed cells to heat that can be created and controlled *via* imposing a magnetic field. Metals used for MNPs design, once incorporated into MOFs, can be applied for MOF-based magnetic therapies, which include, *e.g.*, Fe, Mn, Mg, Ni, and their oxides. For example, Xiang, *et al.* fabricated a MOF-derived porous  $\text{Fe}_3\text{O}_4$ @C nanocomposite and used it to load DOX; the resultant  $\text{Fe}_3\text{O}_4$ @C-PVP@DOX significantly decreased the tumor volume from 2.5 folds of the initio volume to 0.44 and reduced the tumor weight from 0.49 g to 0.10 g without obvious damage to the normal tissues and organs *in vivo* thanks to the combined anti-cancer effect of magnetic-triggered hyperthermia and chemotherapy.<sup>86</sup>

In addition, magnetic nanoparticles have been extensively used for drug delivery due to their attractive properties such as polarization under a robust magnetic force, high coercivity, and non-toxicity, among others.<sup>87</sup> For instance, a Fe-based MOF, namely MIL-100(Fe), was used as the framework to fabricate a magnetic and porous nanocarrier (namely MIL-100 (Fe) @ $\text{Fe}_3\text{O}_4$ @ $\text{SiO}_2$ ) for delivering celecoxib into HeLa cells.<sup>88</sup>

MOF-based magnetic therapies can be coupled with tumor imaging for diagnosis and/or monitoring with the aid of magnetic resonance imaging (MRI). For example, by coating a single hexagonal  $\text{NaYF}_4:\text{Y}_b,\text{Er}$  rare-earth-doped upconversion nanoparticle (UCNP) core with an amino-functionalized Fe carboxylate MOF shell, *i.e.*, MIL-101-NH<sub>2</sub>, Li *et al.* obtained the nanocomposite UCNP@Fe-MIL-101-NH<sub>2</sub> that was capable of combining the NIR optical property of the Fe core and the T2 MRI property of the MOF shell for high-resolution targeted luminescence imaging as demonstrated both *in vitro* and *in vivo*.<sup>89</sup>

### 3.4 MOF-based photodynamic therapies

PDT refers to a minimally invasive treatment modality using photosensitizers that, after being excited by light at a specific wavelength, reacts with  $\text{O}_2$  to generate ROS in the targeted loci for cell killing. Due to the localization of photosensitizers in the tumor lesions and precise light irradiation, PDT has a greater specificity against transformed cells than canonical approaches such as chemotherapies.

Photosensitizers can be either loaded on MOFs through pore loading or be incorporated into the ligands of MOFs. For instance, by loading a porphyrin-derived bridging ligand into



the cavities of a UiO-66 (Hf) MOF, Lu *et al.* obtained a Hf-porphyrin MOF that acted as an effective photosensitizer for PDT against head and neck cancers with reduced likelihood of gaining aggregation and self-quenching due to MOF-enabled particle isolation.<sup>90</sup> On the other hand, by incorporating the pre-designed ligand, *i.e.*, carboxyl-functionalized diiodo-substituted BODIPYs, into the ligand structure of a UiO-66 MOF through solvent-assisted ligand exchange, Wang *et al.* obtained a BODIPY-immobilized zirconium-based MOF with desirable biocompatibility and sufficient singlet oxygen ( $^1\text{O}_2$ ) generation for cancer cell killing.<sup>91</sup>

MOF-based PDT can also synergize with other treatment modalities for enhanced therapeutic. For example, combining PDT with CDT through MOF has shown great therapeutic potential.<sup>92</sup> Yang *et al.* developed lanthanide-doped nanoparticles (LDNPs) coated with Fe/Mn bimetal-doped ZIF-8 (*i.e.*, LDNPs@Fe/Mn-ZIF-8) for NIR-II imaging-guided synergistic PDT/CDT. The LDNPs were synthesized by functionalizing a  $\text{Yb}^{3+}/\text{Ce}^{3+}$ -doped active shell on the NaErF4:Tm core to achieve dual-mode red upconversion and NIR-II downconversion emission in response to NIR irradiation. The dual doping of  $\text{Fe}^{2+}/\text{Mn}^{2+}$  considerably decreased the bandgap of the ZIF-8 photosensitizer, leading to the expansion of ZIF-8 excitation spectrum to the visible light region. In addition,  $\text{Fe}^{2+}/\text{Mn}^{2+}$  ions produced  $\cdot\text{OH}$  *via* the Fenton/Fenton-like reactions to amplify the cell killing effect of PDT once released in the TME on MOF degradation.<sup>20</sup>

### 3.5 MOF-based photothermal therapies

PTT is a cancer treatment approach capable of inducing cancer cell death by heat generated in the tumor tissue on NIR light exposure.<sup>93</sup> A variety of photothermal nanomaterials have been embedded into organic ligands for improved anti-cancer performance that can be classified into three main categories according to their chemical compositions and structures, *i.e.*, metal-doped MOFs, organic-doped MOFs, and polymer-coated MOFs.

Metal-doped MOFs refer to MOFs formed by doping with metal nanoparticles. Photothermal agents (PTAs) with core-shell nanostructures can be loaded on MOFs in this manner. The surface of these hybrids can be easily edited to endow the PTA/MOF with diversified functionalities such as chemophotothermal therapy and controlled drug release. For example, AuNP@ZIF-8 has been used for PTT to resolve the issue of gold nanoparticle (AuNP) aggregation in cancer treatment *in vivo*. Tang *et al.* improved the photothermal effect of AuNP@ZIF-8 under NIR irradiation by modifying the surface structure of AuNPs for enhanced stability that allowed them to be heated up to 54 °C in 5 min under the 808 nm NIR laser.<sup>21</sup>

Organic-doped MOFs are comprised of organic compounds and MOFs, the connection of which is primarily mediated by polymers through covalent or coordination bonds. While metal ions represent the core for reactions, organic compounds provide the space framework of MOF. One type of MOF belonging to this class is ultrathin Cu-TCPP MOF nanosheet that were reported to have a better photothermal conversion

rate than solid photothermal materials due to a larger surface area and faster conversion rate.<sup>94</sup> Nanosheets of this kind include, *e.g.*, graphene oxide, black phosphorus, germanium, boron, metal oxides, and transition metal sulfides.<sup>95,96</sup> It has been reported that Cu-based nanosheets exhibited NIR light absorption properties under 808 nm laser irradiation and possessed ultra-thin structures, allowing them with a broad spectrum and strong light absorption intensity for converting laser energy into heat.

Polymer-coated MOFs refer to MOFs coated by photothermal polymers. Polypyrrole (PPy) and PDA are versatile coating materials commonly used for MOF surface modification for PTT given their strong and wide NIR absorption range. Lin *et al.* reported a PPy-coated Fe-soc-MOF that showed a stronger absorption than Fe-soc-MOF under NIR 808 nm irradiation, and the absorption intensity increased with the increase of Fe-soc-MOF@PPy concentration.<sup>97</sup> Besides, MOFs including, *e.g.*, ZIF-8, MIL-101, and UIO-66, once functionalized with PDA, have been reported to be successfully used for PTT.<sup>98</sup>

There also exist strategies to improve PTT *via* innovative hybridizations. For instance, it has been proposed that photothermal bacterium (PTB) possessed superior photothermal properties under NIR irradiation; by hybridizing ZIF-90 encapsulating photosensitizer methylene blue (ZIF-90/MB) on the surface of living PTB, Chen *et al.* observed enhanced PTT as a result of the accurate release of MB by ZIF-90/MB at mitochondria and the production of  $^1\text{O}_2$  under NIR illumination.<sup>26</sup>

### 3.6 MOF-based sonodynamic therapies

Sonodynamic therapy (SDT) is a sonosensitizer-mediated technology under ultrasound irradiation developed on the basis of PDT.<sup>99</sup> Ultrasound has an extraordinary capacity to penetrate into the target spots with minimal damages to the surrounding healthy tissues.<sup>100,101</sup> While high-intensity ultrasonic irradiation functions similar to PDT that can completely ablate tumors by causing hyperthermia, low-intensity ultrasound irradiation can generate non-thermal biological impact on cells.<sup>102</sup> The most prevailing theory attributes the sonodynamic effect to ROS generation, where  $^1\text{O}_2$  was considered to be responsible for SDT-induced cytotoxicity.<sup>103,104</sup> Similar to PDT, SDT is fast, non-invasive, repeatable, and has low toxicity. It outweighs PDT and may somehow be a complementary technology of PDT in being capable of penetrating through deep tissues.<sup>99</sup> Introducing MOFs to SDT can augment the sonodynamic effect given their large porous structures and superior sonosensitizer-loading ability. The most prevailing way of utilizing MOFs for SDT is to construct MOF-based sonosensitizers; these include MOFs having sonodynamic effects, MOFs loaded with organic sonosensitizers, and MOFs carrying inorganic sonosensitizers.

There are three primary preparation strategies for preparing MOF-based sonosensitizers, *i.e.*, encapsulation, integration, and derivation, among which the most natural way is to simply encapsulating intrinsic sonosensitizers into MOF materials. Zhang *et al.* fabricated hypoxia-responsive sonosensitizer by loading Ce6 to a Cu-MOF ( $\text{Cu}^{2+}$  coordinated with azobenzene-4,4'-dicarboxylic acid).<sup>22</sup> Once entering the TME, Cu-MOF



rapidly degraded and released  $\text{Cu}^{2+}$  and  $\text{Ce}^{6+}$ ; internalized  $\text{Cu}^{2+}$  reacted with local  $\text{GSH}$  and was reduced to  $\text{Cu}^{+}$ , which then reacted with endogenous  $\text{H}_2\text{O}_2$  to produce  $\cdot\text{OH}$  through the Fenton-like reaction; released  $\text{Ce}^{6+}$  further mediated SDT under ultrasound irradiation, leading to effective killing of MCF-7 cells in a minimally invasive manner.<sup>22</sup> Similarly, Huang *et al.* obtained a TME-responsive sonosensitizer by mixing hypoxia-triggered Cu-MOF with an azo initiator AIPH.<sup>105</sup> Given the constituent similarity between sonosensitive metalloporphyrin and MOFs, MOF-based sonosensitizers can be prepared through the direct integration. TCPP, a typical sonosensitizer, is a common candidate for constructing MOFs. Zhang *et al.* synthesized monodispersed Ti-MOF nanoparticles for SDT by coordinatively assembling  $\text{Ti}^{4+}$  and TCPP.<sup>106</sup> Xu *et al.* synthesized spherical-like Zr-MOF, namely PCN-224, through the solvothermal reaction between zirconyl chloride octahydrate and TCPP.<sup>107</sup> MOFs can also be used as a precursor or template to directly or indirectly derive sonosensitizers. Using this strategy, Liang *et al.* prepared the sonosensitizer  $\text{NH}_2\text{-MIL-125(Ti)}$ , and fabricated defect-rich D-MOF(Ti) with enhanced sonosensitizing activity by hydrogenating  $\text{NH}_2\text{-MIL-125(Ti)}$ .<sup>64</sup> Cao *et al.* prepared  $\text{TiO}_2/\text{C}$  sonosensitizers through pyrolyzing MIL-125(Ti) in the air.<sup>108</sup>

## 4 Toxicological characteristics of MOF-based therapeutics

One inevitable yet critical issue that MOFs face is toxicity due to their nano-sizes. The small sizes of nanoparticles enable them to penetrate through physiological barriers, leading to impaired organ functionality as a result of abnormal deposition. In addition, MOFs, once internalized by cells, can mediate toxic effects *via*, *e.g.*, disturbing the integrity of membranes of cells or organelles, interfering with the cellular metabolic processes, producing detrimental reactive oxygen and nitrogen species, and triggering the immune responses.<sup>109</sup> Actually, it is desirable to deliver toxicity to transformed cells once MOFs were internalized by cancer cells as a cancer treatment approach; thus, accurate tumor targeting and prevention against early leakage are relevant issues to be considered for minimized adverse effect in the design of MOF-based therapeutics.

Accordingly, we group factors affecting the distribution, absorption, metabolism and excretion of nanoparticles into two non-mutually exclusive categories following the primary contributions they make to the possible adverse effects caused by MOF-based therapeutics. In specific, we group factors largely affecting the distribution of nanoparticles such as size, agglomeration, metal core, and shape together and name them as 'tissue toxic factors'; and categorize factors primarily influencing cargo release and cell targeting such as chemical stability and surface coating together and name them as 'cell toxic factors'.

### 4.1 Tissue toxic factors

As nanoparticles with sizes ranging from 15 to 200 nm can last for a relatively long period in the circulatory system that enable

them to generate any possible harm to the body, MOFs with the sizes fell into this category are typically considered to be toxic. Large nanoparticles, *i.e.*, with the sizes being  $>200$  nm, are relatively less toxic as they can be detected by the immune system and removed from the blood circulation system. Very small nanoparticles ( $<5\text{--}15$  nm) are also less toxic given that they can be directly excreted through the kidney *via* renal filtration.

Nanoparticle agglomeration is associated with increased particle size and thus affects the potential toxicity of a given MOF. One example of toxicity caused by nanoparticle aggregation is the formation of embolism. Instead of examining the agglomeration potential, one can evaluate the colloidal stability of a given nanoparticle. That is, if a MOF has a good colloidal stability, it is less likely to be toxic due to its unaltered size as a result of homogeneous dispersion in the biological fluids.

The toxicity of a MOF is associated with the type, oxidation state and percentage of its metal core. Very often, the high toxicity of metals (especially heavy metals) is caused by their inability to be biologically degraded and involvement in some essential cellular metabolic processes.

MOFs can be of different shapes such as cube, sphere, tetrahedron, octahedron, and nanocage. As shape can affect the bioactivity, transport, distribution and elimination of a MOF by influencing many of its other features, it is difficult to assess the possible hazardous effect of a given MOF by solely assessing this index.

### 4.2 Cell toxic factors

The targeting efficacy of a given MOF can be affected by its surface coating, which refers to the protein corona formed on the surface of a given nanoparticle as a result of the adsorption of macromolecules such as proteins and lipids.<sup>110</sup> Surface coating can affect the targeting efficacy of a given nanoparticle by interfering with its interactions with cell surface and reducing the amount of MOFs reaching the tumor site *via* triggering strong complement activation. Surface coating is affected by many 'tissue toxic factors' such as the size, with a smaller particle size being associated with a higher level of surface area and a greater proportion of atoms being exposed to the cellular environment.

Early leakage of anti-cancer agents due to the chemical instability of a given MOF may lead to insufficient tumor targeting and, correspondingly, toxicity to the healthy cells. Among the varied factors affecting the chemical stability of MOFs, the varied pH values of the different locations in the human body have a huge impact, imposing a great challenge to the design of pH-sensitive MOFs. The strength of the coordination bonds between the metal core and organic linkers can be estimated according to the hard and soft acids and bases principle. In specific, hard metals such as  $\text{Ti}^{4+}$ ,  $\text{Fe}^{3+}$ ,  $\text{Cr}^{3+}$  and  $\text{Zr}^{4+}$ , form stable bonds with hard linkers such as carboxylates; soft metals such as  $\text{Zn}^{2+}$  and  $\text{Cu}^{2+}$  form stable bonds with soft linkers such as imidazolates, pyrazolates, and triazolate. While a more acidic environment triggers the decomposition of MOFs based on soft constituents by fostering the competition between metal ions



and protons for the binding with the organic linker,<sup>111</sup> a more basic environment enables the degradation of MOFs based on hard components by initiating a successive replacement of organic linkers by hydroxide ions.<sup>112,113</sup> Another critical factor influencing the chemical stability of MOFs is the nuclearity of their inorganic building unit. For instance, ZIF-8(Zn) is stable at pH >6, MOF-74(Zn) only starts to decompose when pH drops to 3,<sup>114</sup> and UiO-66(Zr) and NU-1000(Zr) are highly stable attributing to the high nuclearity of their Zr6-metal clusters.<sup>115</sup>

## 5 Conclusion

Given the high flexibility of MOFs in surface modification and the relatively weak coordination bonds formed between metal ions and organic ligands, MOFs can be designed for controlled drug release in response to various external stimuli such as pH, redox level, magnetic field, light, heat and ultrasound, which means that they are stable unless being exposed to the corresponding stimuli. This holds a great promise in the biomedical sector for, *e.g.*, therapeutic design, as these MOFs may not only act for targeted drug delivery but also add flexibilities to a plethora of cancer treatment strategies such as magnetic therapy, PDT, PTT and SDT. Importantly, these MOFs make therapeutics targeting tumors, the TME, or both possible and in a controlled manner. So far, physical stimuli such as magnetism, light, heat, sound have all been successfully utilized in the control of MOF-based cargo release, would it be also possible that other sources of stimulus such as electricity function as well? In addition, cold atmospheric plasma (CAP), a fourth state of matter capable of generating various reactive oxygen and nitrogen species, has demonstrated its unique selectivity against cancer cells (*i.e.*, specifically killing transformed cells without harming their healthy peers). Would this innovative form of stimulus (*i.e.*, oxidative stimuli) be able to trigger MOFs to collapse for cargo release or to create any other sort of anti-cancer synergies with MOFs? These are all interesting topics that may initiate novel research directions in the nano-field and possibly lead to the generation of innovative techniques for effective cancer control.

## Conflicts of interest

The authors declare no conflict of interest.

## References

- 1 R. L. Siegel, K. D. Miller, N. S. Wagle and A. Jemal, *Ca-Cancer J. Clin.*, 2023, **73**, 17–48.
- 2 L. Jiao, J. Y. R. Seow, W. S. Skinner, Z. U. Wang and H.-L. Jiang, *Mater. Today*, 2019, **27**, 43–68.
- 3 H. Deng, S. Grunder, K. E. Cordova, C. Valente, H. Furukawa, M. Hmadeh, F. Gándara, A. C. Whalley, Z. Liu, S. Asahina, H. Kazumori, M. O'Keeffe, O. Terasaki, J. F. Stoddart and O. M. Yaghi, *Science*, 2012, **336**, 1018–1023.
- 4 R. W. Sun, M. Zhang, D. Li, Z. F. Zhang, H. Cai, M. Li, Y. J. Xian, S. W. Ng and A. S. Wong, *Chemistry*, 2015, **21**, 18534–18538.
- 5 P. Gao, M. Shi, R. Wei, W. Pan, X. Liu, N. Li and B. Tang, *Chem. Commun. (Camb.)*, 2020, **56**, 924–927.
- 6 J. Chen, Y. Zhu and S. Kaskel, *Angew Chem., Int. Ed.*, 2021, **60**, 5010–5035.
- 7 C. Liu, B. Liu, J. Zhao, Z. Di, D. Chen, Z. Gu, L. Li and Y. Zhao, *Angew Chem., Int. Ed.*, 2020, **59**, 2634–2638.
- 8 T. Simon-Yarza, M. Gimenez-Marques, R. Mrimi, A. Mielcarek, R. Gref, P. Horcajada, C. Serre and P. Couvreur, *Angew Chem., Int. Ed.*, 2017, **56**, 15565–15569.
- 9 I. Abanades Lazaro, S. Haddad, S. Saccà, C. Orellana-Tavira, D. Fairen-Jimenez and R. S. Forgan, *Chem*, 2017, **2**, 561–578.
- 10 K. Ni, G. Lan, C. Chan, B. Quigley, K. Lu, T. Aung, N. Guo, P. La Riviere, R. R. Weichselbaum and W. Lin, *Nat. Commun.*, 2018, **9**, 2351.
- 11 H. M. Meng, X. X. Hu, G. Z. Kong, C. Yang, T. Fu, Z. H. Li and X. B. Zhang, *Theranostics*, 2018, **8**, 4332–4344.
- 12 P. Horcajada, T. Chalati, C. Serre, B. Gillet, C. Sebrie, T. Baati, J. F. Eubank, D. Heurtaux, P. Clayette, C. Kreuz, J. S. Chang, Y. K. Hwang, V. Marsaud, P. N. Bories, L. Cynober, S. Gil, G. Ferey, P. Couvreur and R. Gref, *Nat. Mater.*, 2010, **9**, 172–178.
- 13 M. H. Teplensky, M. Fantham, P. Li, T. C. Wang, J. P. Mehta, L. J. Young, P. Z. Moghadam, J. T. Hupp, O. K. Farha, C. F. Kaminski and D. Fairen-Jimenez, *J. Am. Chem. Soc.*, 2017, **139**, 7522–7532.
- 14 H. Zheng, Y. Zhang, L. Liu, W. Wan, P. Guo, A. M. Nystrom and X. Zou, *J. Am. Chem. Soc.*, 2016, **138**, 962–968.
- 15 X. Lian, Y. Fang, E. Joseph, Q. Wang, J. Li, S. Banerjee, C. Lollar, X. Wang and H. C. Zhou, *Chem. Soc. Rev.*, 2017, **46**, 3386–3401.
- 16 M. X. Wu and Y. W. Yang, *Adv. Mater.*, 2017, **29**, 1606134.
- 17 D. P. Ling, H. H. Li, W. S. Xi, Z. Wang, A. Bednarkiewicz, S. T. Dibaba, L. Y. Shi and L. N. Sun, *J. Mater. Chem. B*, 2020, **8**, 1316–1325.
- 18 L. G. Li, X. X. Yang, H. Z. Xu, T. T. Yu, Q. R. Li, J. Hu, X. C. Peng, N. Han, X. Xu, N. N. Chen, X. Chen, J. M. Tang and T. F. Li, *Adv. Healthcare Mater.*, 2023, **12**, 2301561.
- 19 B. Yang, L. Ding, H. Yao, Y. Chen and J. Shi, *Adv. Mater.*, 2020, **32**, e1907152.
- 20 C. S. Li, J. Ye, X. Yang, S. Liu, Z. Y. Zhang, J. Wang, K. F. Zhang, J. T. Xu, Y. J. Fu and P. P. Yang, *ACS Nano*, 2022, **16**, 18143–18156.
- 21 Y. T. Li, J. Jin, D. W. Wang, J. W. Lv, K. Hou, Y. L. Liu, C. Y. Chen and Z. Y. Tang, *Nano Res.*, 2018, **11**, 3294–3305.
- 22 K. Zhang, X. D. Meng, Z. Yang, H. F. Dong and X. J. Zhang, *Biomaterials*, 2020, **258**, 120278.
- 23 X. C. Cai, X. G. Bao and Y. L. Wu, *Pharmaceutics*, 2022, **14**, 2641.
- 24 Z. Zong, G. H. Tian, J. L. Wang, C. B. Fan, F. L. Yang and F. Guo, *Pharmaceutics*, 2022, **14**, 2790.
- 25 J. Munawar, M. S. Khan, S. E. Z. Syeda, S. Nawaz, F. A. Janjhi, H. Ul Haq, E. U. Rashid, T. Jesionowski and M. Bilal, *Inorg. Chem. Commun.*, 2023, **147**, 110145.



26 Q. W. Chen, X. H. Liu, J. X. Fan, S. Y. Peng, J. W. Wang, X. N. Wang, C. Zhang, C. J. Liu and X. Z. Zhang, *Adv. Funct. Mater.*, 2020, **30**, 1909806.

27 Z. X. Zhou, M. Vazquez-Gonzalez and I. Willner, *Chem. Soc. Rev.*, 2021, **50**, 4541–4563.

28 D. Hanahan, *Cancer Discovery*, 2022, **12**, 31–46.

29 T. T. Wang, D. G. Wang, J. P. Liu, B. Feng, F. Y. Zhou, H. W. Zhang, L. Zhou, Q. Yin, Z. W. Zhang, Z. L. Cao, H. J. Yu and Y. P. Li, *Nano Lett.*, 2017, **17**, 5429–5436.

30 F. M. Zhang, H. Dong, X. Zhang, X. J. Sun, M. Liu, D. D. Yang, X. Liu and J. Z. Wei, *ACS Appl. Mater. Interfaces*, 2017, **9**, 27332–27337.

31 S. Javanbakht, M. Pooreesmaeil and H. Namazi, *Carbohydr. Polym.*, 2019, **208**, 294–301.

32 Y. Guo, B. Yan, Y. Cheng and L. Mu, *J. Coord. Chem.*, 2019, **72**, 262–271.

33 A. Cabrera-Garcia, E. Checa-Chavarria, E. Rivero-Buceta, V. Moreno, E. Fernandez and P. Botella, *J. Colloid Interface Sci.*, 2019, **541**, 163–174.

34 H. Chen, Z. Y. Chen, Y. Kuang, S. Li, M. Zhang, J. Liu, Z. G. Sun, B. B. Jiang, X. Q. Chen and C. Li, *Colloids Surf., B*, 2018, **167**, 407–414.

35 Y. Zhang, L. Wang, L. Liu, L. Lin, F. Liu, Z. G. Xie, H. Y. Tian and X. S. Chen, *ACS Appl. Mater. Interfaces*, 2018, **10**, 41035–41045.

36 H. Y. Zhang, Q. Li, R. L. Liu, X. K. Zhang, Z. H. Li and Y. X. Luan, *Adv. Funct. Mater.*, 2018, **28**, 1802830.

37 Y. Wang, J. H. Yan, N. C. Wen, H. J. Xiong, S. D. Cai, Q. Y. He, Y. Q. Hu, D. M. Peng, Z. B. Liu and Y. F. Liu, *Biomaterials*, 2020, **230**, 119619.

38 H. F. Zhao, S. J. Hou, X. D. Zhao and D. H. Liu, *J. Chem. Eng. Data*, 2019, **64**, 1851–1858.

39 S. Kouuser, A. Hezam, M. J. N. Khadri and S. A. Khanum, *J. Porous Mater.*, 2022, **29**, 663–681.

40 P. Raju, P. Arivalagan and S. Natarajan, *J. Photochem. Photobiol., B*, 2020, **203**, 111774.

41 D. Mete, E. Yemeztaslica and G. Sanli-Mohamed, *J. Drug Delivery Sci. Technol.*, 2023, **82**, 104362.

42 M. R. Song, D. Y. Li, F. Y. Nian, J. P. Xue and J. J. Chen, *J. Mater. Sci.*, 2018, **53**, 2351–2361.

43 Y. Y. Liu, Z. H. Li, S. Y. Zou, C. B. Lu, Y. Xiao, H. Bai, X. L. Zhang, H. B. Mu, X. Y. Zhang and J. Y. Duan, *Int. J. Biol. Macromol.*, 2020, **155**, 103–109.

44 S. X. Yu, S. Y. Wang, Z. K. Xie, S. Y. Yu, L. Li, H. F. Xiao and Y. D. Song, *Colloids Surf., B*, 2021, **203**, 111759.

45 J. Z. Zhang, M. S. Han, J. Zhang, M. Abdalla, P. Sun, Z. M. Yang, C. Zhang, Y. Liu, C. Chen and X. Y. Jiang, *Int. J. Pharm.*, 2023, **640**, 123025.

46 S. L. Wang, H. S. Wu, K. Sun, J. Z. Hu, F. H. Chen, W. Liu, J. Chen, B. W. Sun and A. M. S. Hossain, *New J. Chem.*, 2021, **45**, 3271–3279.

47 C. L. Yang, S. K. Tiwari, L. S. Guo, G. H. An, H. M. Zheng, J. F. Huang, L. Jiang, Z. H. Bai, Y. Q. Zhu and N. N. Wang, *Front. Oncol.*, 2023, **13**, 1110909.

48 L. Kennedy, J. K. Sandhu, M. E. Harper and M. Cuperlovic-Culf, *Biomolecules*, 2020, **10**, 1429.

49 Y. B. Wang, W. B. Wu, D. Mao, C. Teh, B. Wang and B. Liu, *Adv. Funct. Mater.*, 2020, **30**, 2002431.

50 Y. Liu, Y. R. Wang, X. Guan, Q. Wu, M. J. Zhang, P. Cui, C. Wang, X. W. Chen, X. W. Meng and T. C. Ma, *ACS Appl. Mater. Interfaces*, 2023, **15**, 26484–26495.

51 C. X. Lin, H. L. He, Y. Q. Zhang, M. Y. Xu, F. Tian, L. Li and Y. X. Wang, *RSC Adv.*, 2020, **10**, 3084–3091.

52 H. D. Cornell, Y. M. Zhu, S. Ilic, N. E. Lidman, X. Z. Yang, J. B. Matson and A. J. Morris, *Chem. Commun.*, 2022, **58**, 5225–5228.

53 H. M. Bi and X. J. Han, *Chem. Phys. Lett.*, 2018, **706**, 455–460.

54 Y. Wang, Y. Miao, G. Li, M. Su, X. Chen, H. Zhang, Y. Zhang, W. Jiao, Y. He, J. Yi, X. Liu and H. Fan, *Mater. Today Adv.*, 2020, **8**, 100119.

55 M. Attia, R. D. Glickman, G. Romero, B. L. Chen, A. J. Brenner and J. Y. Ye, *J. Drug Delivery Sci. Technol.*, 2022, **76**, 103770.

56 J. C. Li, X. R. Yu, Y. Y. Jiang, S. S. He, Y. Zhang, Y. Luo and K. Y. Pu, *Adv. Mater.*, 2021, **33**, 2003458.

57 X. X. Yao, B. R. Yang, C. Z. Li, Q. J. He and W. L. Yang, *Chem. Eng. J.*, 2023, **453**, 139888.

58 J. Qiao, C. Cheng, D. Li and L. Qi, *J. Mater. Chem. B*, 2023, **11**, 6428–6434.

59 A. Karmakar, P. G. M. Mileo, I. Bok, S. B. Peh, J. Zhang, H. Yuan, G. Maurin and D. Zhao, *Angew. Chem., Int. Ed.*, 2020, **59**, 11003–11009.

60 X. Chen, H. Zhang, M. Zhang, Y. Zou, S. Zhang and Y. Qu, *Chem. Commun. (Camb.)*, 2020, **56**, 1960–1963.

61 Y. M. Xiang, J. L. Lu, C. Y. Mao, Y. Z. Zhu, C. F. Wang, J. Wu, X. M. Liu, S. L. Wu, K. Y. H. Kwan, K. M. C. Cheung and K. W. K. Yeung, *Sci. Adv.*, 2023, **9**, eadf0854.

62 K. L. Liu, Z. Q. Jiang, F. G. Zhao, W. Z. Wang, F. Jakle, N. Wang, X. Y. Tang, X. D. Yin and P. K. Chen, *Adv. Mater.*, 2022, **34**, 2206594.

63 X. T. Pan, W. W. Wang, Z. J. Huang, S. Liu, J. Guo, F. R. Zhang, H. J. Yuan, X. Li, F. Y. Liu and H. Y. Liu, *Angew. Chem., Int. Ed.*, 2020, **59**, 13557–13561.

64 S. Liang, X. Xiao, L. X. Bai, B. Liu, M. Yuan, P. A. Ma, M. L. Pang, Z. Y. Cheng and J. Lin, *Adv. Mater.*, 2021, **33**, 2100333.

65 Y. L. Yan, X. X. Yang, N. Han, Y. H. Liu, Q. J. Liang, L. G. Li, J. Hu, T. F. Li and Z. J. Xu, *J. Nanobiotechnol.*, 2023, **21**, 204.

66 X. R. Kong, Z. J. He, Y. Zhang, Y. L. Fang, D. Z. Liu, H. Wu, J. B. Ji, Y. W. Xi, L. Ye, X. Y. Yang and G. X. Zhai, *Chem. Eng. J.*, 2023, **468**, 143729.

67 M. Parsaei and K. Akhbari, *Inorg. Chem.*, 2022, **61**, 5912–5925.

68 N. D. Bikiaris, N. M. Ainali, E. Christodoulou, M. Kostoglou, T. Kehagias, E. Papasouli, E. N. Koukaras and S. G. Nanaki, *Nanomaterials-Basel*, 2020, **10**, 2490.

69 P. H. Wu, P. F. Cheng, W. Kaveevivitchai and T. H. Chen, *Colloids Surf., B*, 2023, **225**, 113264.

70 G. S. Chen, J. Y. Luo, M. R. Cai, L. Y. Qin, Y. B. Wang, L. L. Gao, P. Q. Huang, Y. C. Yu, Y. M. Ding, X. X. Dong, X. B. Yin and J. Ni, *Molecules*, 2019, **24**, 3369.



71 Y. Wang, G. R. Williams, Y. Zheng, H. Guo, S. Chen, R. Ren, T. Wang, J. Xia and L.-M. Zhu, *J. Colloid Interface Sci.*, 2023, **651**, 76–92.

72 Y. W. Li, Y. Wei, Y. Huang, G. Qin, C. Q. Zhao, J. S. Ren and X. G. Qu, *Small*, 2023, **19**, 2301519.

73 L. H. Du, H. Z. He, Z. C. Xiao, H. Xiao, Y. C. An, H. H. Zhong, M. Z. Lin, X. C. Meng, S. S. Han and X. T. Shuai, *Small*, 2022, **18**, 2107732.

74 Z. Rao, Y. Xia, Q. Jia, Y. Zhu, L. Wang, G. Liu, X. Liu, P. Yang, P. Ning, R. Zhang, X. Zhang, C. Qiao and Z. Wang, *J. Nanobiotechnol.*, 2023, **21**, 265.

75 X. D. Gong, J. Wang, L. L. Yang, L. J. Li, X. Y. Gao, X. Sun, J. F. Bai, J. C. Liu, X. Pu and Y. D. Wang, *Small*, 2023, **19**, 2301497.

76 G. Li, X. Y. Lu, S. X. Zhang, J. B. Zhang, X. G. Fu, M. M. Zhang, L. S. Teng and F. Y. Sun, *ACS Appl. Mater. Interfaces*, 2023, **15**, 31285–31299.

77 Z. B. Yang, Y. Luo, Y. A. Hu, K. C. Liang, G. He, Q. Chen, Q. G. Wang and H. R. Chen, *Adv. Funct. Mater.*, 2021, **31**, 2007991.

78 C. Szabo, *Nat. Rev. Drug Discovery*, 2007, **6**, 917–935.

79 Y. J. Li, J. J. Dang, Q. J. Liang and L. C. Yin, *ACS Cent. Sci.*, 2019, **5**, 1044–1058.

80 Y. Q. Zheng, B. C. Yu, L. K. De La Cruz, M. R. Choudhury, A. Anifowose and B. H. Wang, *Med. Res. Rev.*, 2018, **38**, 57–100.

81 T. Yang, A. N. Zelikin and R. Chandrawati, *Adv. Sci.*, 2018, **5**, 1701043.

82 H. B. Ji, S. N. Kim, C. R. Kim, C. H. Min, J. H. Han, M. J. Kim, C. Lee and Y. B. Choy, *Biomater. Adv.*, 2023, **145**, 213268.

83 M. T. Xia, Y. Yan, H. Y. Pu, X. N. Du, J. Y. Liang, Y. N. Sun, J. N. Zheng and Y. Yuan, *Chem. Eng. J.*, 2022, **442**, 136295.

84 P. Das, M. Colombo and D. Prosperi, *Colloids Surf., B*, 2019, **174**, 42–55.

85 Y. T. Qin, H. Peng, X. W. He, W. Y. Li and Y. K. Zhang, *ACS Appl. Mater. Interfaces*, 2019, **11**, 34268–34281.

86 Z. Xiang, Y. Qi, Y. Lu, Z. Hu, X. Wang, W. Jia, J. Hu, J. Ji and W. Lu, *J. Mater. Chem. B*, 2020, **8**, 8671–8683.

87 M. D. Nguyen, H. V. Tran, S. Xu and T. R. Lee, *Appl. Sci. (Basel)*, 2021, **11**, 11301.

88 A. Lajevardi, M. H. Sadr, A. Badiei and M. Armaghan, *J. Mol. Liq.*, 2020, **307**, 112996.

89 Y. Li, J. Tang, L. He, Y. Liu, Y. Liu, C. Chen and Z. Tang, *Adv. Mater.*, 2015, **27**, 4075–4080.

90 K. Lu, C. He and W. Lin, *J. Am. Chem. Soc.*, 2014, **136**, 16712–16715.

91 W. Wang, L. Wang, Z. Li and Z. Xie, *Chem. Commun. (Camb.)*, 2016, **52**, 5402–5405.

92 Y. Cheng, C. Wen, Y. Q. Sun, H. Yu and X. B. Yin, *Adv. Funct. Mater.*, 2021, **31**, 2104378.

93 S. Nomura, Y. Morimoto, H. Tsujimoto, M. Arake, M. Harada, D. Saitoh, I. Hara, E. Ozeki, A. Satoh, E. Takayama, K. Hase, Y. Kishi and H. Ueno, *Sci. Rep. UK*, 2020, **10**, 9765.

94 J. A. Ibacache, J. A. Valderrama, V. Arancibia, C. Theoduloz, G. G. Muccioli and J. Benites, *J. Chil. Chem. Soc.*, 2016, **61**, 3191–3194.

95 Y. A. Cheon, J. H. Bae and B. G. Chung, *Langmuir*, 2016, **32**, 2731–2736.

96 S. Lee, Y. Cho, H. K. Song, K. T. Lee and J. Cho, *Angew. Chem., Int. Ed.*, 2012, **51**, 8748–8752.

97 X. C. Cai, X. R. Deng, Z. X. Xie, Y. S. Shi, M. L. Pang and J. Lin, *Chem. Eng. J.*, 2019, **358**, 369–378.

98 J. Feng, Z. Xu, P. Dong, W. Q. Yu, F. Liu, Q. Y. Jiang, F. Wang and X. Q. Liu, *J. Mater. Chem. B*, 2019, **7**, 994–1004.

99 F. F. Yang, J. Dong, Z. F. Li and Z. H. Wang, *ACS Nano*, 2023, **17**, 4102–4133.

100 R. Breitkopf, B. Treml and S. Rajsic, *Diagnostics*, 2022, **12**, 1405.

101 R. Abdelnaby, K. A. Mohamed, A. Elgenidy, Y. T. Sonbol, M. M. Bedewy, A. M. Aboutaleb, M. A. Ebrahim, I. Maallem, K. T. Dardeer, H. A. Heikal, H. M. Gawish and J. Zschuntzsch, *Cells-Basel*, 2022, **11**, 600.

102 J. Dong, Z. H. Wang, F. F. Yang, H. Q. Wang, X. J. Cui and Z. F. Li, *Adv. Colloid Interface Sci.*, 2022, **305**, 102683.

103 X. W. Wang, X. Y. Zhong, L. X. Bai, J. Xu, F. Gong, Z. L. Dong, Z. J. Yang, Z. J. Zeng, Z. Liu and L. Cheng, *J. Am. Chem. Soc.*, 2020, **142**, 6527–6537.

104 Z. L. Li, J. Han, L. D. Yu, X. Q. Qian, H. Xing, H. Lin, M. C. Wu, T. Yang and Y. Chen, *Adv. Funct. Mater.*, 2018, **28**, 1800145.

105 Y. Sun, J. Cao, X. Wang, C. Zhang, J. L. Luo, Y. Q. Zeng, C. Zhang, Q. Y. Li, Y. Zhang, W. Xu, T. Zhang and P. T. Huang, *ACS Appl. Mater. Interfaces*, 2021, **13**, 38114–38126.

106 T. Zhang, Y. Sun, J. Cao, J. L. Luo, J. Wang, Z. Q. Jiang and P. T. Huang, *J. Nanobiotechnol.*, 2021, **19**, 315.

107 Q. B. Xu, G. T. Zhan, Z. L. Zhang, T. Y. Yong, X. L. Yang and L. Gan, *Theranostics*, 2021, **11**, 1937–1952.

108 J. Cao, Y. Sun, C. Zhang, X. Wang, Y. Q. Zeng, T. Zhang and P. T. Huang, *Acta Biomater.*, 2021, **129**, 269–279.

109 Y. Zhang, Y. H. Bai, J. B. Jia, N. N. Gao, Y. Li, R. N. Zhang, G. B. Jiang and B. Yan, *Chem. Soc. Rev.*, 2014, **43**, 3762–3809.

110 M. P. Monopoli, C. Åberg, A. Salvati and K. A. Dawson, *Nat. Nanotechnol.*, 2012, **7**, 779–786.

111 C. Y. Sun, C. Qin, X. L. Wang, G. S. Yang, K. Z. Shao, Y. Q. Lan, Z. M. Su, P. Huang, C. G. Wang and E. B. Wang, *Dalton Trans.*, 2012, **41**, 6906–6909.

112 E. Bellido, M. Guillevic, T. Hidalgo, M. J. Santander-Ortega, C. Serre and P. Horcajada, *Langmuir*, 2014, **30**, 5911–5920.

113 C. G. Piscopo, A. Polyzoidis, M. Schwarzer and S. Loebbecke, *Microporous Mesoporous Mater.*, 2015, **208**, 30–35.

114 J. Schnabel, R. Ettlinger and H. Bunzen, *Chemnanomat*, 2020, **6**, 1229–1236.

115 Y. J. Chen, P. Li, J. A. Modica, R. J. Drout and O. K. Farha, *J. Am. Chem. Soc.*, 2018, **140**, 5678–5681.

